Applied Nanoscience (2023) 13:4873–4882
https://doi.org/10.1007/s13204-022-02640-1

ORIGINAL ARTICLE

Synthesis of zinc molybdate nanostructures via an alternative green approach

O. A. Diyuk[1] · V. O. Zazhigalov[1] · N. V. Diyuk[2] · S. A. Sergiienko[3] · V. V. Permyakov[4] · S. M. Shcherbakov[5] · N. D. Shcherban[6]

Received: 31 May 2022 / Accepted: 21 September 2022 / Published online: 8 October 2022

Abstract

The low temperature method of synthesis of zinc molybdate nanostructures from oxides by hydrothermal, ultrasonic treatment, and conventional stirring was proposed. The synthesis of $ZnMoO_4$ from oxides in an aqueous medium at room temperature confirmed the thermodynamic possibility of this process. Ultrasonic or hydrothermal treatment led to an acceleration of the $ZnMoO_4$ synthesis process. Alternative synthesis methods and conventional co-precipitation methods from soluble salts were compared. It was shown that an alternative synthesis leads to the formation of the $ZnMoO_4{\cdot}0.8H_2O$ phase. DTA method showed that $ZnMoO_4{\cdot}0.8H_2O$ loses crystallization water in two stages up to 320 °C and $ZnMoO_4$ was formed. All $ZnMoO_4$ samples synthesized by alternative methods have higher S_{BET} than $ZnMoO_4$ synthesized by a solid-state method. It was shown by SEM and TEM that $ZnMoO_4$ synthesized by hydrothermal treatment, ultrasonic treatment, and stirring have similar nanorod structure. Consequently, it was shown that the application of alternative synthesis methods allows to obtain the $ZnMoO_4$ nanostructures at low temperature avoiding environmental pollution.

Keywords Zinc molybdate nanostructures · Green synthesis · Hydrothermal treatment · Ultrasonic treatment

Introduction

Water pollution is known to be one of the top ten environmental problems. Therefore, the creation of the synthesis method meeting the main requirements of "green chemistry" is an incredibly urgent task (Anastas et al. 1998).

$ZnMoO_4$ is known as an industrial white pigment with anti-corrosion performance (Bhanvase et al. 2015; Karekar et al. 2018; Sheng et al. 2021), as well as an industrial smoke suppressant (Jr et al. 2020; Zhang et al. 2019). Moreover, $ZnMoO_4$ has been recently shown to be among promising luminescent materials (Zhai et al. 2017a; Cavalcante et al. 2012; Degoda et al. 2017; Hizhnyia et al. 2019; Wang et al. 2017; Tiwari et al. 2020; Yadav et al. 2019), bolometers, scintillation humidity sensors, gas sensors (Bhanvase et al. 2015; Beeman et al. 2012; Chernyak et al. 2013; Gironi et al. 2010; Edwin Suresh Raj et al. 2002; Shahri et al. 2013), photocatalysts, and catalysts for partial hydrocarbons oxidation (Oudghiri-Hassani et al. 2018; Wang et al. 2017; Zazhigalov et al. 2019), anode materials (Fei et al. 2017; Masood et al. 2020; Xue et al. 2016; Wang et al. 2020). However, all known methods of $ZnMoO_4$ producing cannot be considered environmentally friendly due to the fact that they require

✉ O. A. Diyuk
diyukhelen@ukr.net

1 Institute for Sorption and Problems of Endoecology, National Academy of Sciences of Ukraine, 13 General Naumov Street, Kyiv 03164, Ukraine

2 Taras Shevchenko National University of Kyiv, 60 Volodymyrska Street, Kyiv 01033, Ukraine

3 Department of Materials and Ceramics Engineering, University of Aveiro, CICECO-Aveiro Institute of Materials, 3810-193 Aveiro, Portugal

4 Institute of Geological Sciences, National Academy of Sciences of Ukraine, 55-b O.Gonchar Str., Kyiv 01054, Ukraine

5 M.G.Kholodny Institute of Botany, National Academy of Sciences of Ukraine, 2 Tereshchenkivska Str., Kyiv 01004, Ukraine

6 L.V. Pisarzhevsky Institute of Physical Chemistry, National Academy of Sciences of Ukraine, 31 pr. Nauky, Kyiv 03028, Ukraine

high temperature in the case of solid-state (SS) synthesis (da Silva Filho et al. 2020; Diyuk et al. 2021; Zhang et al. 2010; Hizhnyia et al. 2019; Tiwari et al. 2020; Jin et al. 2019) or a large amount of water to remove polluting ions in the case of co-precipitation synthesis (Ait ahsaine et al. 2015; Zhang et al. 2010; Hizhnyia et al. 2019). In addition, the SS synthesis prevents the formation of the $ZnMoO_4$ nanostructure. On the other hand, the co-precipitation synthesis provides not more than 50% yield of the desired product which additionally can be contaminated with by-products (Diyuk et al. 2021; Jin et al. 2019).

Application of alternative synthesis methods can help solve this problem. For instance, a novel mechanochemical method of β-$ZnMoO_4$ synthesis from oxides in an air medium was described (Zazhigalov et al. 2016). Several papers have reported the application of ultrasonic (Bhanvase et al. 2015; Karekar et al. 2015; Lovisa et al. 2018; Patel et al. 2013) or hydrothermal equipment (Sheng et al. 2021; Cavalcante et al. 2012; Zhang et al. 2010; Jiang et al. 2014) for the preparation of molybdenum salt. However, the use of starting reagents (metal salts) and additional substances in these procedures leads to water pollution. Thereby, hydrothermal and ultrasonic synthesis methods allow to obtain novel improved $ZnMoO_4$ nanostructures; however, does not solve the environmental problem of water pollution by ions. Additionally, one-hour ultrasonic treatment of the corresponding oxides in aqueous medium was reported to lead to the mixture of products (α-$ZnMoO_4$, α-MoO_3, β-Mo_8O_{23}, and β-$ZnMoO_4$) (Sachuk et al. 2017; Zazhigalov et al. 2017, 2019). However, in these publications, the potential (thermodynamic) possibility of the interaction of oxides at low temperatures was not considered. In the current paper a concept of the interaction of poorly soluble oxides in aqueous medium resulting in the formation of nanostructured $ZnMoO_4$ was proposed and the experimental results confirming this hypothesis are presented.

Experimental

The samples preparation

For the preparation of the zinc molybdate samples by a conventional co-precipitate method $(NH_4)_6Mo_7O_{24}{\cdot}4H_2O$ 2.354 g and $Zn(NO_3)_2{\cdot}6H_2O$ 3.959 g with the molar ratio of 1:7 were used. Each of these salts was solved in 100 ml of distilled water in separate beakers. Then zinc nitrate solution was gradually added to the ammonium molybdate solution. Afterward, some NH_4OH as a precipitating agent was added. After that, HNO_3 solution was added to get the pH of ca. 7. The sample synthesized by a co-precipitation method was washed 5 times with 500 ml of deionized water. After that, the sample was dried at 100 °C and 300 °C and marked as ZnMoO_c-p_100 and ZnMoO_c-p_300, respectively.

The solid-state synthesis was realized according to the procedure described in (Diyuk et al. 2021) where the physical–chemical properties of the obtained samples were reported. Some of the properties of this sample are presented in this paper, and the sample is labeled as ZnMoO_SS.

The used alternative methods of synthesis were based on the interaction of metal oxides in aqueous medium:

1. The conventional stirring (with a magnetic stirrer) of the oxides mixture in the water medium at room temperature was performed with the duration of 7 days. This synthesis was carried out according to the modified procedure applied for the successful synthesis of $ZnMo_2O_7{\cdot}5H_2O$ (Grzywaa et al. 2007). [In the original source (Grzywaa et al. 2007) the duration of the synthesis was one month]. The mixture of ZnO 3.61 g and MoO_3 6.39 g (1:1 molar ratio) was placed into a beaker and 200 ml of water was added. The suspension was stirred for 6 h during each day at room temperature (a long time is essential due to the low solubility of both components). The sample was dried at 100 °C and 300 °C and labeled as ZnMoO_st_100 and ZnMoO_st_300, respectively.
2. The second synthesis method was performed according to the procedure described in (Diyuk et al. 2021). The mixture of ZnO 3.61 g and MoO_3 6.39 g with the molar ratio of 1:1 was placed into a glass beaker and 80 ml of water was added. The ultrasonic (US) treatment of the oxides mixture was carried out for 20 min at room temperature using an UZDN-A ultrasonic dispersant operating in an acoustic cavitations mode at a frequency of 22 kHz. After synthesis the samples were dried at 100 °C and 300 °C and labeled as ZnMoO_US_100 and ZnMoO_US_300, respectively.
3. The hydrothermal treatment of the oxides mixture (molar ratio equal to 1:1) was realized by a similar procedure described in (Zazhigalov et al. 2014). The synthesis was carried out in a stainless-steel laboratory autoclave with a volume of 45 ml and an inserted teflon test tube of 18 ml. The oxides ZnO – 1.44 g and MoO_3 – 2.56 g were mixed and placed into a teflon insert, and 15 ml of water was added. The autoclave was heated at 170 °C for 3 h. The pressure in the autoclave was 0.8 MPa. After synthesis, the sample was dried at 100 °C or 300 °C and marked as ZnMoO_HT_100 and ZnMoO_HT_300, respectively.

Characterization of the samples

The phase composition of the prepared samples was determined using Bruker D8 Advance diffractometer equipped with Cu Kα ($\lambda = 0.15406$ nm) X-ray source in the range of

2Θ 5°–70°. For the analysis of the samples composition and morphology, a scanning electron microscope (SEM JSM6490 LV, JEOL, Japan) with an integrated system for electron microprobe analysis INCA Energy based on energy-dispersive and wavelength-dispersive spectrometers (EDS + WDS, OXFORD, United Kingdom) with HKL Channel system was applied. Transmission electron microscopy (TEM) for the investigation of the morphology and size of the initial and obtained materials was carried out on a transmission electron microscope JEM-1200 EX (JEOL, Japan). Nitrogen adsorption isotherms at –196 °C were obtained using Quantachrome NOVA- 220e Gas Sorption Analyzer. Differential thermal analysis (DTA) was performed on Paulik-Paulik-Erdey Derivatograph Q instrument with independent channels of registration for TG, DTG and DTA. The experiments were carried out in air in the temperature range of 25–500 °C at the heating rate of 10 °C/min. The sample weight was 200 mg.

Results and discussion

XRD

XRD patterns of the samples prepared by a co-precipitation method are presented in Fig. 1. The synthesis using the initial salts ($(NH_4)_6Mo_7O_{24}\cdot 4H_2O$ and $Zn(NO_3)_2\cdot 6H_2O$) leads to the formation of zinc molybdate (ZnMoO_c-p_100). Since the synthesis was performed with the Zn to Mo atomic ratio equal to 1, the formation of the product with a similar Zn to Mo ratio was expected. At the same time according to XRD analysis the main reflexes of the obtained product correspond to $Zn_5Mo_2O_{11}\cdot 5H_2O$ (JCPDS card no. 00–030-14–86). The formation of $Zn_5Mo_2O_{11}\cdot 5H_2O$ from the initial salts makes it impossible to obtain pure $ZnMoO_4$ after calcination Eq. (1). According to this equation the final product contains the mixture of $ZnMoO_4$ and ZnO.

$$Zn_5Mo_2O_{11}\cdot 5H_2O \rightarrow 2ZnMoO_4 + 3ZnO + 5H_2O \quad (1)$$

At the same time, the XRD (Fig. 1b) contains reflexes of the single α-$ZnMoO_4$ phase (JCPDS No 00–035-0765). Thereby, the obtained ZnO can be presented by the amorphous form or small nanocrystals which cannot be detected by XRD. It is necessary to note that in some publications, the samples after co-precipitation synthesis were not studied and XRD patterns of the product after calcination were demonstrated only (for example, Ait ahsaine et al. 2015). In this paper, the final product was detected as pure $ZnMoO_4$. In this case, one cannot be sure that the single phase $ZnMoO_4$ was obtained. In (Zhai et al. 2017a) it was announced that the co-precipitation method led to the formation of the

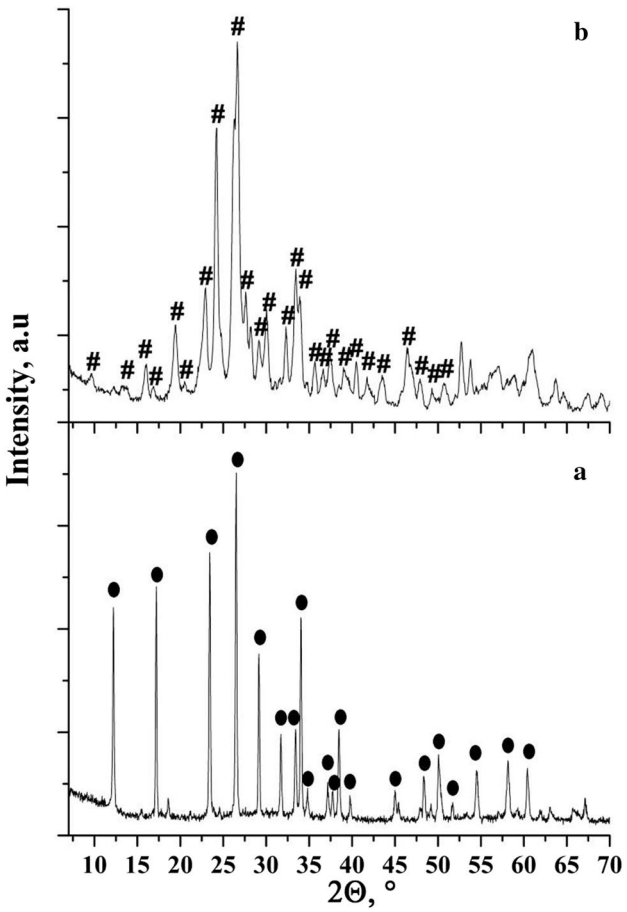

Fig. 1 X-ray diffraction patterns: **a** ZnMoO_c-p_100, **b** ZnMoO_c-p_300, were ● - $Zn_5Mo_2O_{11}\cdot 5H_2O$ and # - $ZnMoO_4$

precursor (without its XRD identification) turning after calcination into a single $ZnMoO_4$ phase with nanowire structure. However, the presented in the paper SEM images demonstrate, in addition to the nanowire structure, the presence of a large number of particles with a flake structure probably corresponding to amorphous ZnO phase. In another paper (Zhai et al. 2017b) pentazinc dimolybdate pentahydrate was identified as a synthesis product and further calcination of $Zn_5Mo_2O_{11}\cdot 5H_2O$ in the temperature range from 150 to 300 °C was shown to lead to the formation of the $ZnMoO_4$ phase (XRD). However, in this case, as in our synthesis, the formation of ZnO according to Eq. (1) was not detected by X-ray diffraction analysis. Therefore, the obtained results and literature data show that the co-precipitation synthesis allows to obtain the $ZnMoO_4$ phase, however, the presence of amorphous zinc oxide cannot be excluded. On the other hand, soluble molybdenum compounds should remain in the water, reducing the productivity of the synthesis and increasing environmental pollution.

Figure 2a shows the XRD patterns of the sample obtained by the stirring of the corresponding oxides mixture in water

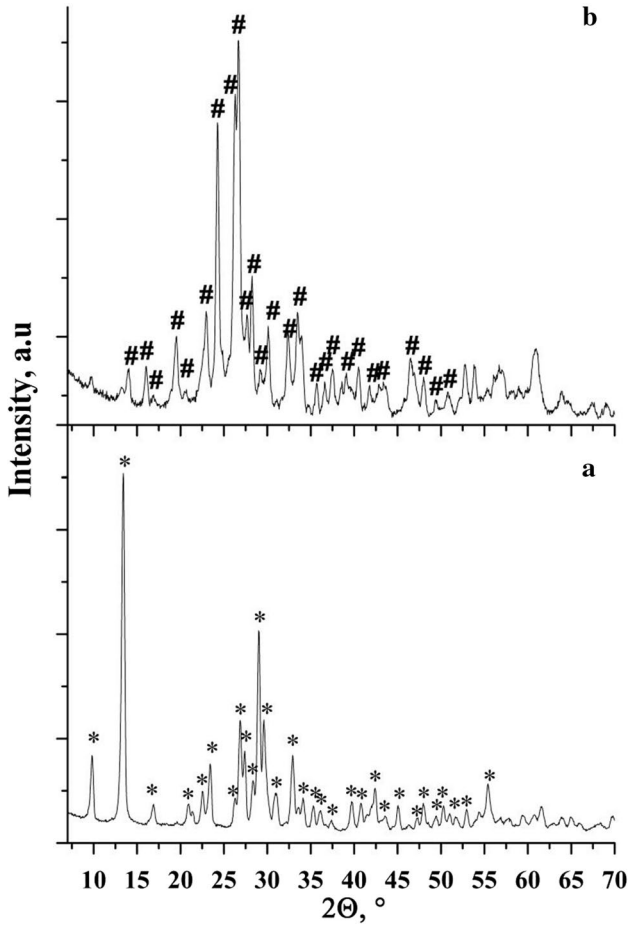

Fig. 2 X-ray diffraction patterns: **a** ZnMoO_st_100, **b** ZnMoO_st_300 were * - $ZnMoO_4 \cdot 0.8H_2O$ and # - $ZnMoO_4$

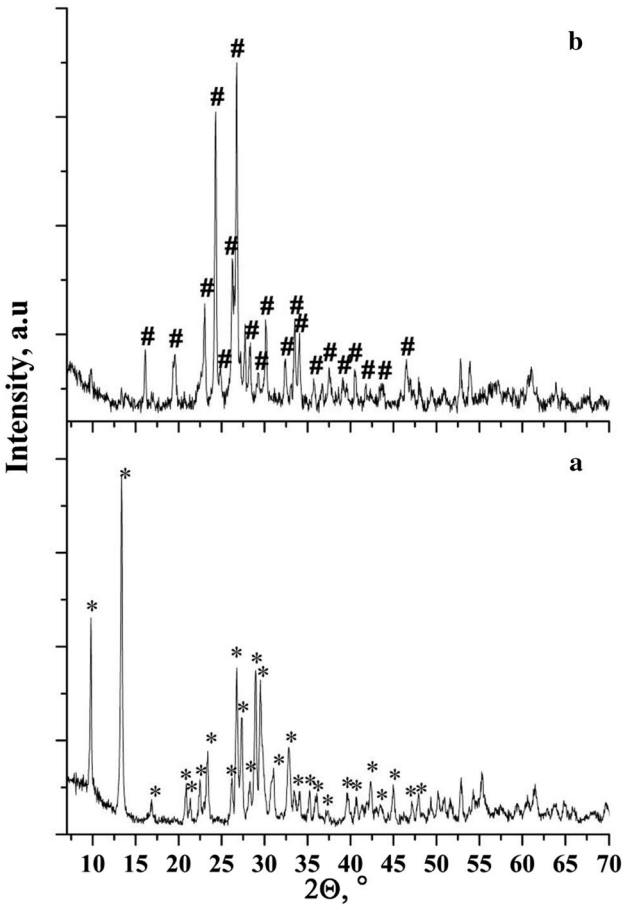

Fig. 3 X-ray diffraction patterns: **a** ZnMoO_US_100, **b** ZnMoO_US_300 were * - $ZnMoO_4 \cdot 0.8H_2O$ and # - $ZnMoO_4$

medium using a magnetic stirrer at room temperature. All the signals of ZnMoO_st_100 correspond to $ZnMoO_4 \cdot 0.8H_2O$ (JCPDS 00-025-1025). All the peaks in the XRD pattern of ZnMoO_st_300 (Fig. 2b) can be indexed according to the standard peaks of $ZnMoO_4$ without any other phases. Since the reaction between the initial oxides (ZnO and MoO_3) with the formation of zinc molybdate occurs in aqueous medium at room temperature, it can be considered as a spontaneous process. It should be noted that it is a very slow process. The reason for a long-term reaction is kinetic difficulties and problems with the contact between the particles of the initial reagents. The initial oxides ZnO and MoO_3 are characterized by the poor solubility of 0.004 g/l and 1.066 g/l respectively at 18 °C, therefore, the reaction is too slow. As a result, two different ways can be proposed to speed up the process rate. The first method is connected with an increase of the dispersion of the initial compounds and their intensive mixing (US treatment). The second one is to increase the solubility of oxides by increasing the reaction temperature (hydrothermal treatment). Both these approaches were studied in the current work. In Fig. 3a, b X-ray diffraction patterns of the sample obtained after US treatment during 20 min are presented. All reflexes of ZnMoO_US_100 correspond to $ZnMoO_4 \cdot 0.8H_2O$ (Fig. 3a) and the reflexes of ZnMoO_US_300 allow to identify the sample as $ZnMoO_4$. These data are in a good agreement with the results presented in (Diyuk et al. 2021) and differ from the XRD data reported in (Zazhigalov et al. 2019, 2017; Sachuk et al. 2017), where the formation of α-$ZnMoO_4$ α-MoO_3, β-Mo_8O_{23} and β-$ZnMoO_4$ mixture after the US treatment of ZnO and MoO_3 during 1 h was registered. This can be connected with some different US treatment conditions.

Thermal treatment leads to the formation of $ZnMoO_4$ phase. It can be concluded that the application of US treatment significantly (more than 100 times) speeds up the process of the formation of $ZnMoO_4 \cdot 0.8H_2O$ compared to the conventional stirring confirming one of the suggested hypothesis.

X-ray diffraction patterns of ZnMoO_HT_100 and ZnMoO_HT_300 are presented in Fig. 4. The main reflexes correspond to $ZnMoO_4 \cdot 0.8H_2O$ except two peaks at $2\Theta = 19.7$ and 24.34 which can be ascribed to $ZnMoO_4$.

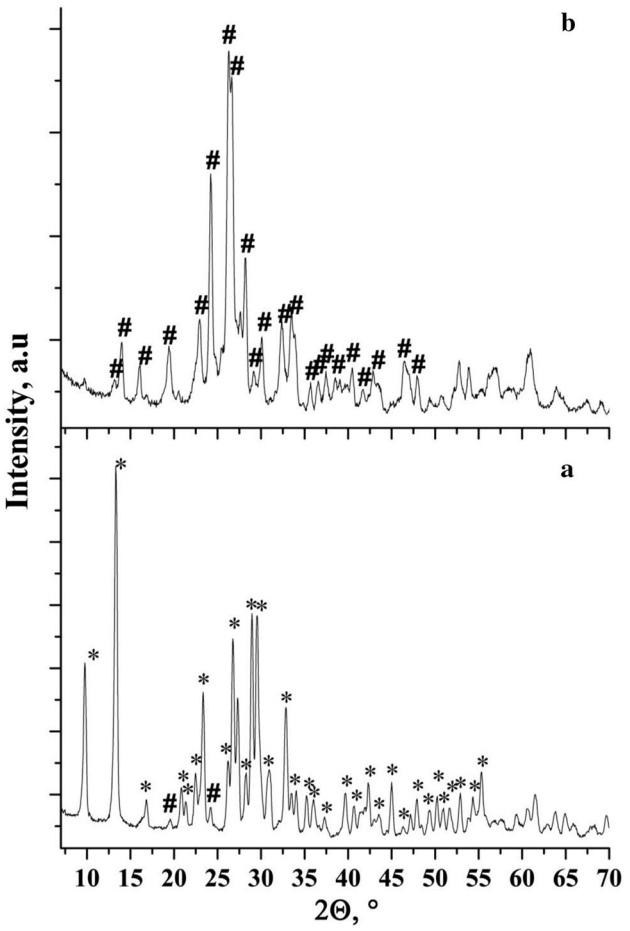

Fig. 4 X-ray diffraction patterns: **a** ZnMoO_HT_100, **b** ZnMoO_HT_300 were * - $ZnMoO_4 \cdot 0.8H_2O$, # - $ZnMoO_4$

This fact indicates that a small amount of $ZnMoO_4$ was obtained (less than 3% according to the ratio of the main peaks) as the result of HT synthesis. After the calcination of $ZnMoO_4 \cdot 0.8H_2O$ all the reflexes in XRD pattern correspond to $ZnMoO_4$. These results confirm our hypothesis that HT treatment can positively influence the process kinetics.

Thereby, the obtained results show that a traditional co-precipitation method can lead to the formation of by-products. Otherwise, alternative synthesis methods such as conventional stirring with a magnetic stirrer, ultrasonic and hydrothermal treatment lead to the formation of the $ZnMoO_4 \cdot 0.8H_2O$ phase with further transformation into a single $ZnMoO_4$ phase after calcination.

SEM

SEM image of the product obtained by a traditional co-precipitation method from the metal salts (ZnMoO_cp_300) is presented in Fig. 5a. This sample consists of two types of particles: the nanorod structures characteristic for $ZnMoO_4$ (Zhai et al. 2017a; Zhang et al. 2010; Fei et al. 2017; Karekar et al. 2015; Wang et al. 2017; Keereeta et al. 2014) and some amount of friable structure probably corresponded to ZnO formed according to Eq. 1. The SEM image of the initial mixture of oxides used for synthesis is shown in Fig. 5b. EDX analysis showed the presence of a fine ZnO powder that surrounds massive MoO_3 particles. It is shown (Fig. 5c1) that the stirring of the oxides mixture in an aqueous medium leads to the formation of rod structure particles. At the same time on the sample surface, the presence of small particles with different morphology can be observed. The data of EDX analysis show that in the places with a rod structure, the distribution of elements is uniform, while in the places containing these small particles a large amount of molybdenum was detected (Fig. 5c2). This result indicates an incomplete transformation of the initial reagents (in particular molybdenum oxide). The obtained data confirmed the conditions of this synthesis reported by (Grzywaa et al. 2007) about one-month duration for the preparation of the pure product. In accordance to our hypothesis, ultrasonic treatment allows to obtain the product with homogeneous nanorod structure (Fig. 5d) corresponded to $ZnMoO_4$ formation. Such a strong reduction in the synthesis duration leading to the formation of a pure product can be explained by the elimination of kinetic limitations due to an increase the dispersion of the initial compounds as a result of US treatment. Synthesis of zinc molybdate using hydrothermal treatment also leads to the formation of nanorod structure (Fig. 5e). EDX analysis of ZnMoO_US_300 and ZnMoO_HT_300 samples demonstrates equimolar and uniform distribution of elements in these samples.

TEM

TEM-images of the initial ZnO and MoO_3 oxides are presented in Fig. 6a, b. The initial molybdenum oxide consists of the large particles in different forms: parallelogram, triangular, and others (Fig. 6a). The initial zinc oxide is composed of small circular particles collected in agglomerates (Fig. 6b). The TEM images of $ZnMoO_4$ display that all the samples synthesized by alternative methods have similar rod-like structure (Fig. 6c–e). These particles have the width equal to 20–200 nm, and the length up to 2 μm. All TEM images of the prepared zinc molybdate well agree with the SEM images and confirm the formation of the rod-like structure.

Nitrogen ad(de)sorption

The results of nitrogen ad(de)sorption for the samples synthesized by an alternative approach and SS method where the $ZnMoO_4$ phase was obtained are presented in Table 1. The samples synthesized by alternative methods have 10–15

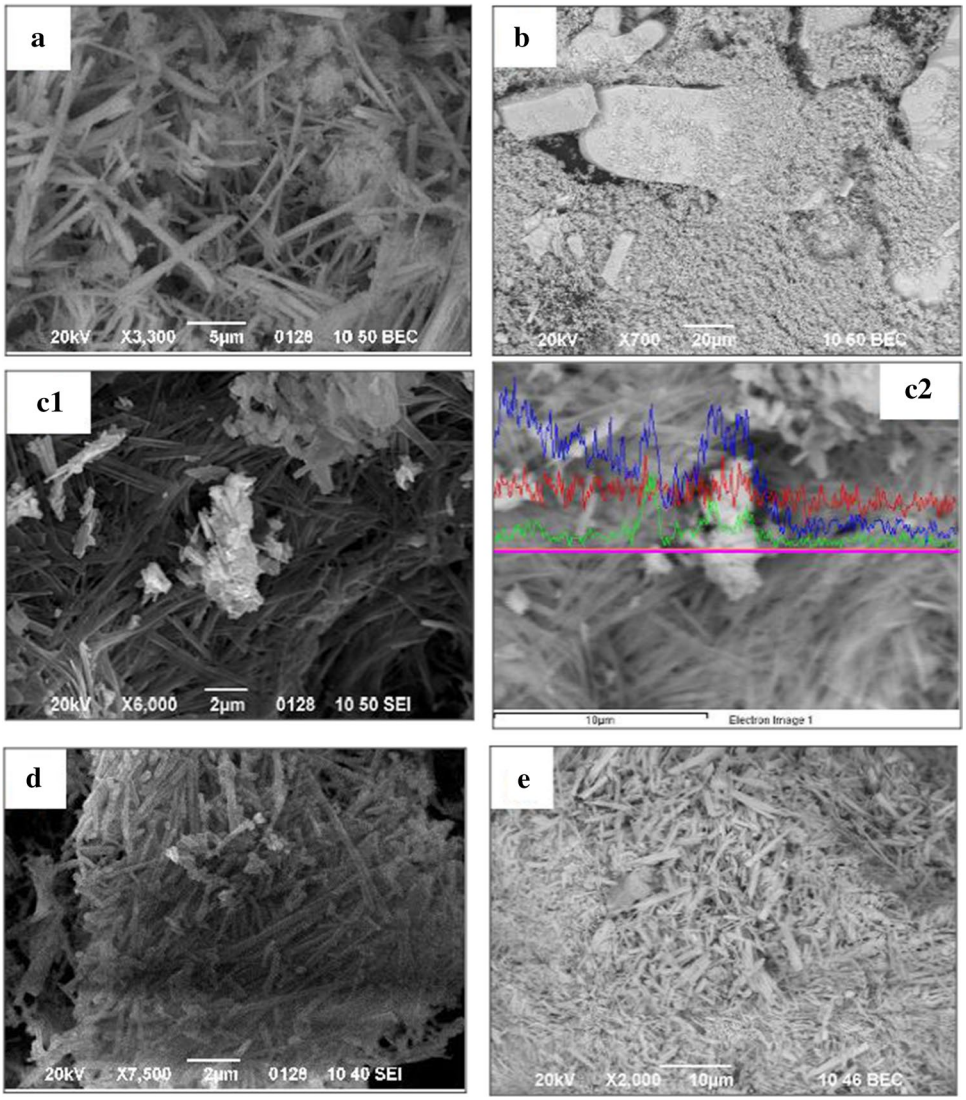

Fig. 5 SEM images of the samples: **a** ZnMoO_c-p_300, **b** initial mixture of MoO_3 and ZnO, **c** 1,2) ZnMoO_st_300 with EDXA where blue line – Mo, red line – Zn and green line – O, **d** ZnMoO_US_300, **e** ZnMoO_HT_300

times higher S_{BET} value than the samples synthesized by the SS method (Diyuk et al. 2021). Milder synthesis conditions lead to the formation of the sample with a larger specific surface area and more developed porosity. It should be noted that the samples ZnMoO_st and ZnMoO_US have very close values of both S_{BET} and V_{Σ}. On the other hand, the synthesis of $ZnMoO_4$ due to an increase in temperature leads to a noticeable decrease in both parameters.

DTA

The initial mixture of oxides (ZnO and MoO_3) has a total weight loss of 1% in the TG curve and no peaks in DTA curves (image is not shown). It can be connected with non-porous structure of the initial oxides and corresponding low quantity of adsorbed water.

In Fig. 7a TG, DTA, and DTG curves of ZnMoO_c-p_100 with the $Zn_5Mo_2O_{11}{\cdot}5H_2O$ phase detected by XRD are presented. There is a weight loss of 10% in the temperature range of 240–330 °C accompanied by only one endothermic peak at 275 °C. These data are close to the theoretical calculation of lost crystalline water equal to 11 wt% according to the presented Eq. (1). Despite the large number of publications devoted to the synthesis of $ZnMoO_4$, only a few of them reported DTA studies. For all the samples synthesized by alternative methods, two stages of weight loss were observed (Fig. 7b–d). The first weight loss was observed at about 50–230 °C and the second one – 250–320 °C. The total weight loss varies from 4.6% for ZnMoO_HT_100 up to 7% for ZnMoO_st_100 (Fig. 7b–d). The theoretically calculated weight loss of 0.8 molecules of crystal water during the formation of $ZnMoO_4$ from $ZnMoO_4{\cdot}0.8H_2O$ is equal to 6%, therefore both of these stages of weight loss can be connected with this process. However, the first stage of $ZnMoO_4{\cdot}0.8H_2O$ weight loss can be also associated with the water adsorbed in the pores. The second stage of

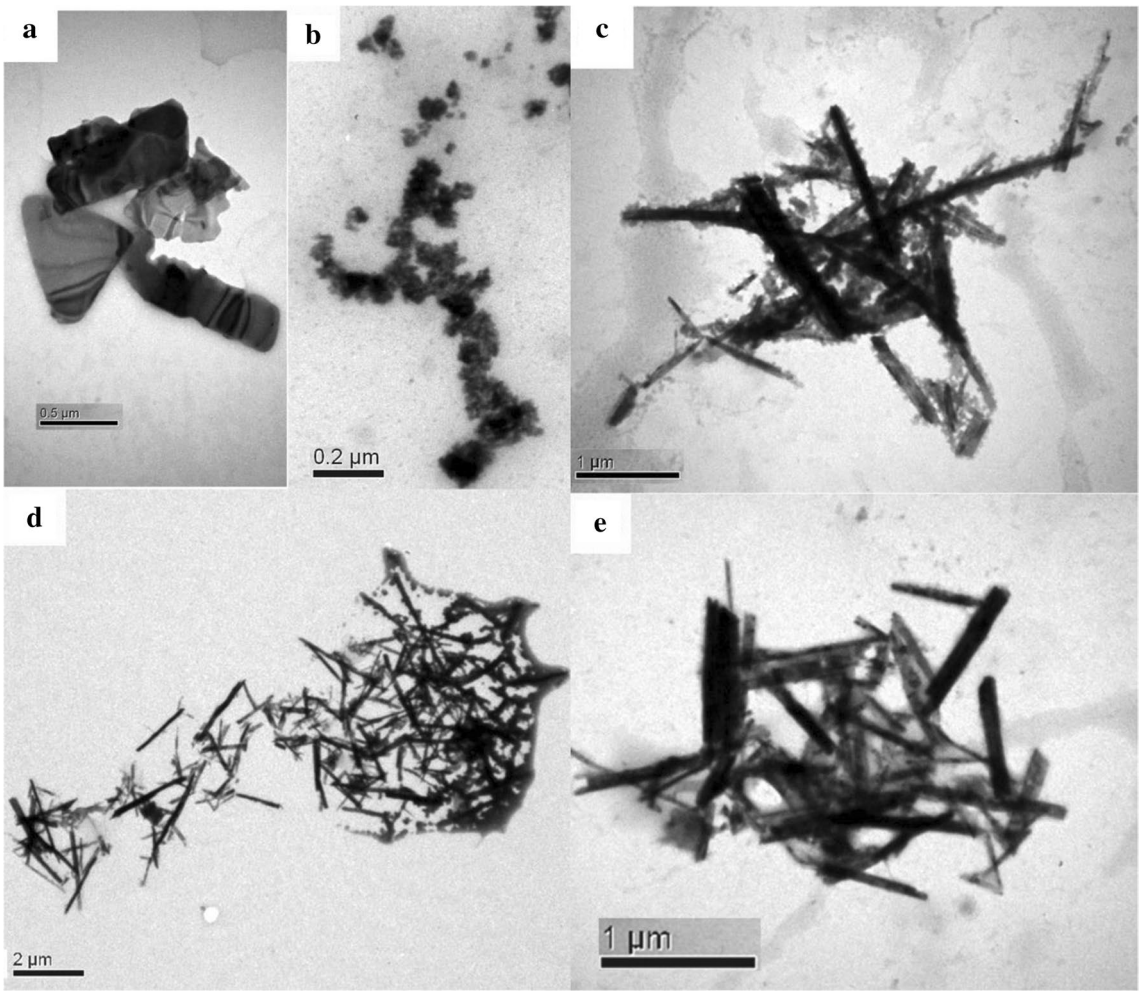

Fig. 6 TEM images: **a** MoO_3, **b** ZnO, **c** ZnMoO_st_300, **d** ZnMoO_US_300, **e** ZnMoO_HT_300

Table 1 Porosity parameters of the $ZnMoO_4$ samples

Sample	ZnMoO_SS	ZnMoO_st_300	ZnMoO_US_300	ZnMoO_HT_300
S_{BET}, m^2/g	0.6	9	8	6
V_{Σ}, cm^3/g	0.01	0.123	0.115	0.05
Ref	Diyuk et al. (2021)	This paper	This paper	This paper

weight loss at a temperature of 250–320 °C is the same for all samples (2–3%) and associated only with the removal of crystalline water. Our results are in a good agreement with (Zhang et al. 2010) where $ZnMoO_4 \cdot 0.8H_2O$ was prepared by a co-precipitate method using hydrothermal treatment. In this study the total weight loss was 5.27%. As can be seen from Fig. 7d, ZnMoO_HT_100 has the lowest weight loss among all other samples. It may be due to the relatively high synthesis temperature and high pressure leading to the partial formation of $ZnMoO_4$, already at the stage of synthesis, which was confirmed by X-ray diffraction analysis (Fig. 4a). The application of hydrothermal treatment, both in the co-precipitate synthesis from salt (Zhang et al. 2010) and hydrothermal synthesis from oxides (this paper) leads to the lower values of the amount of crystal water determined by DTA method compared to theoretically calculated one.

Conclusions

The possibility of the $ZnMoO_4 \cdot 0.8H_2O$ phase formation under standard conditions (NIST: atmospheric pressure, temperature 20 °C) by the mixing of the corresponding oxides in an aqueous medium at room temperature

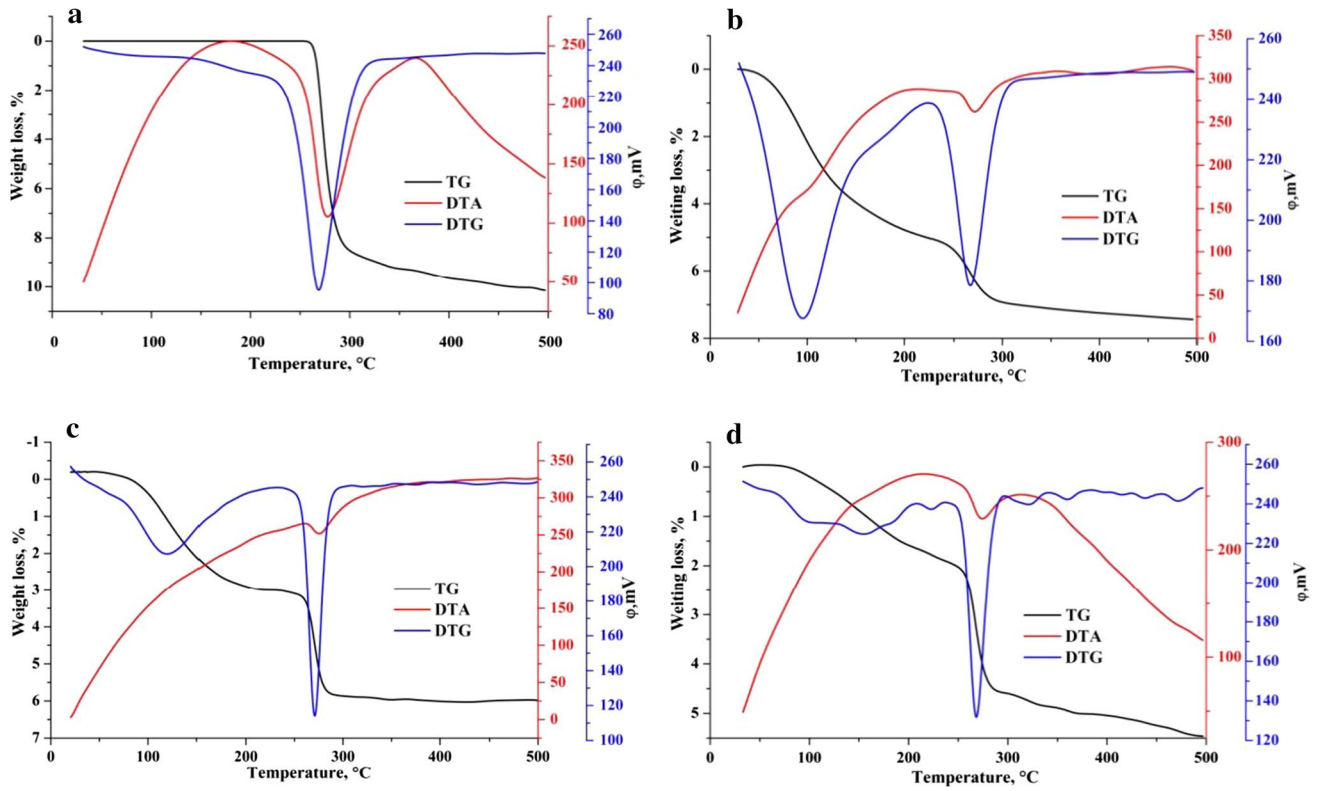

Fig. 7 DTA, TG, and DTG **a** ZnMoO_c-p_100, **b** ZnMoO_st_100, **c** ZnMoO_US_100, **d** ZnMoO_HT_100

was demonstrated. All alternative procedures lead to the formation of crystalline hydrate $ZnMoO_4 \cdot 0.8H_2O$ with a nanorod structure. This fact indicates the irreplaceable key role of water in overcoming the kinetic difficulties of the process during the low-temperature synthesis of the salt from oxides in an aqueous medium. It was shown that the kinetic difficulties can be overcome by an increase in the reagents dispersion and enhancing the mixing using ultrasonic treatment or by an increase in the solubility of oxides by heating in the case of hydrothermal treatment. At the same time, the method of oxides treatment in water medium has some impact on the properties of the product. It is worth noting that after heating $ZnMoO_4 \cdot 0.8H_2O$ transforms into $ZnMoO_4$ with the same nanorod structure. As a result, green synthesis of zinc molybdate from oxides at the temperature lower by 600 °C compared to the conventional SS synthesis was developed. In comparison with the traditional co-precipitation synthesis, the studied methods allow to obtain $ZnMoO_4$ with the yield of ca. 100% and practically without water pollution.

Acknowledgements This work was financially supported by NASU Program "New functional substances and materials of chemical production" (project 13-21).

Declarations

Conflict of interest The authors declare that they have no competing interests.

References

Ait ahsaine H, Zbair M, Ezahri M, Benlhachemi A, Arab M, Bakiz B, Guinneton F, Gavarri J-R, (2015) Rietveld refinements, impedance spectroscopy and phase transition of the polycrystalline $ZnMoO_4$ ceramics. J Ceram Int 41:15193–15201. https://doi.org/10.1016/j.ceramint.2015.08.094

Anastas PT, Warner JC (1998) Green chemistry: theory and practice. Oxford University Press, Oxford: New York

Beeman JW, Bellini F, Capelli S, Cardani L, Casali N, Dafinei I, Di Domizio S, Ferroni F et al (2012) $ZnMoO_4$: A promising bolometer for neutrinoless double beta decay searches. Astropart Phys 35:813–820. https://doi.org/10.1016/j.astropartphys.2012.02.013

Bhanvase BA, Darda NS, Veerkar NC, Shende AS, Satpute SR, Sonawane SH (2015) Ultrasound assisted synthesis of PANI/$ZnMoO_4$ nanocomposite for simultaneous improvement in anticorrosion, physico-chemical properties and its application in gas sensing. Ultrason Sonochem 24:87–97. https://doi.org/10.1016/j.ultsonch.2014.11.009

Cavalcante LS, Sczancoski JC, Li MS, Longo E, Varela JA (2012) β-$ZnMoO_4$ microcrystals synthesized by the surfactant-assisted hydrothermal method: Growth process and photoluminescence properties. Colloids Surf Physicochem Eng Asp 396:346–351. https://doi.org/10.1016/j.colsurfa.2011.12.021

Chernyak DM, Danevich FA, Degoda VYa, Dmitruk IM, Ferri F, Galashov EN, Giuliani A, et al (2013) Optical, luminescence and thermal properties of radiopure $ZnMoO_4$ crystals used in scintillating bolometers for double beta decay search. Nucl Instrum Methods Phys Res 729:856–863. https://doi.org/10.1016/j.nima.2013.07.088

da Silva Filho JG, Saraiva GD, de Castro AJR, Neto VOS, Saraiva-Souza A, Silva CB, Lima JA, Teixeira AMR, Freire PTC, Paraguassu W, de Sousa FF (2020) Vibrational spectroscopy study and ab initio calculation on $ZnMoO_4$ system. J Mol Struct 1206:127776. https://doi.org/10.1016/j.molstruc.2020.127776

Degoda VYa, Kogut YaP, Moroz IM, Danevich FA, Nasonov SG, Makarov EP, Shlegel VN, (2017) Temperature dependence of luminescence intensity in $ZnMoO_4$ crystal. Mater Res Bull 89:139–149. https://doi.org/10.1016/j.materresbull.2017.01.010

Diyuk OA, Zazhigalov VA, Shcherban ND, Permyakov VV, Diyuk NV, Shcherbakov SM, Sachuk OV, Dulian P (2021) Kinetics of $ZnMoO_4{\cdot}0.8H_2O$ and α-$ZnMoO_4$ Formation at Ultrasonic Treatment of ZnO and MoO_3 Mixture. Nanocomposit Nanostruct Appl 263:87–101. https://doi.org/10.1007/978-3-030-74741-1_6

Fei J, Sun Q, Cui Y, Li J, Huang J (2017) Sodium carboxyl methyl cellulose and polyacrylic acid binder with enhanced electrochemical properties for $ZnMoO_4{\cdot}0.8H_2O$ anode in lithium ion batteries. J Electroanalyt Chem 804:158–164. https://doi.org/10.1016/j.jelechem.2017.09.061

Gebre SH (2021) Recent developments of supported and magnetic nanocatalysts for organic transformations: an up-to-date review. Appl Nanosci. https://doi.org/10.1007/s13204-021-01888-3

Gironi L, Arnaboldi C, Beeman JW, Cremonesi O, Danevich FA, Degoda VYa, Ivleva LI, et al (2010) Performance of $ZnMoO_4$ crystal as cryogenic scintillating bolometer to search for double beta decay of molybdenum. J Instrum 5:1–12. https://doi.org/10.1088/1748-0221/5/11/P11007

Grzywaa M, Łasochaa W, Surgac W (2007) Synthesis, characterization and crystal structure of zinc dimolybdate pentahydrate $ZnMo_2O_7{\cdot}5H_2O$. J Solid State Chem 180:1590–1594. https://doi.org/10.1016/j.jssc.2007.02.024

Hizhnyi Yu, Zatovsky I, Nedilko S, Boiko R, Li J, Han W, Klyui NI (2019) Origin of luminescence in $ZnMoO_4$ crystals: Insights from spectroscopic studies and electronic structure calculations. J Lumin 211:127–137. https://doi.org/10.1016/j.jlumin.2019.03.031

Jiang YR, Lee WW, Chen KT, Wang MC, Chang KH, Chen CC (2014) Hydrothermal synthesis of b-$ZnMoO_4$ crystals and their photocatalytic degradation of Victoria Blue R and phenol. J Taiwan Inst Chem Eng 45:207–218. https://doi.org/10.1016/j.jtice.2013.05.007

Jin Y, Pang T (2019) Highly efficient green upconversion luminescence of $ZnMoO_4$:Yb^{3+}/Er^{3+}/Li^+ for accurate temperature sensing. Spectrochim Acta A Mol Biomol Spectrosc 211:306–312. https://doi.org/10.1016/j.saa.2018.12.018

Junior AR, Innocentini-Mei LH (2021) Synthesis of copper(II)-zinc-molybdenum compounds as smoke suppressants for PVC compositions. Fire Mater 45:396–405. https://doi.org/10.1002/fam.2817

Karekar SE, Bhanvase BA, Sonawane SH, Deosarkar MP, Pinjari DV, Pandit AB (2015) Synthesis of zinc molybdate and zinc phosphomolybdate nanopigments by an ultrasound assisted route: Advantage over conventional method. Chem Eng Process 87:51–59. https://doi.org/10.1016/j.cep.2014.11.010

Karekar SE, Bagale UD, Sonawane SH, Bhanvase BA, Pinjari DV (2018) A smart coating established with encapsulation of Zinc Molybdate centred nanocontainer for active corrosion protection of mild steel: release kinetics of corrosion inhibitor. Compos Interfaces 25:785–808. https://doi.org/10.1080/09276440.2018.1439631

Keereeta Y, Thongtem T, Thongtem S (2014) Effect of medium solvent ratios on morphologies and optical properties of a-$ZnMoO_4$, b-$ZnMoO_4$ and $ZnMoO_4{\cdot}0.8H_2O$ crystals synthesized by microwave-hydrothermal/solvothermal method. Superlattices Microstruct 69:253–264. https://doi.org/10.1016/j.spmi.2014.02.011

Khajuria S, Ladol J, Sanotra S et al (2016) Green hydrothermal synthesis and optical properties of γ-Gd_2S_3 nanoparticles. Appl Nanosci 6:653–658. https://doi.org/10.1007/s13204-015-0478-7

Lovisa LX, Oliveira MC, Andrés J, Gracia L, Lid MS, Longo E, Tranquilin RL, Paskocimas CA, Bomio MRD, Motta FV (2018) Structure, morphology and photoluminescence emissions of $ZnMoO_4$: RE $^{3+}$=Tb^{3+} - Tm^{3+} - x Eu^{3+} (x = 1, 1.5, 2, 2.5 and 3 mol%) particles obtained by the sonochemical method. J Alloys Compd 750:55–70. https://doi.org/10.1016/j.jallcom.2018.03.394

Masood KB, Parte G, Jain N, Dwivedi PK, Kumar P, Shelke MV, Patel RP, Singh J (2020) Electrochemical performance of pre-lithiated $ZnMoO_4$ and r-GO@$ZnMoO_4$ composite anode for lithium-ion battery application. J Taiwan Inst Chem Eng 112:60–66. https://doi.org/10.1016/j.jtice.2020.07.009

Oudghiri-Hassani H, Rakass S, Abboudi M, Mohmoud A, Wadaani FA (2018) Preparation and characterization of α-zinc molybdate catalyst: efficient sorbent for methylene blue and reduction of 3-nitrophenol. Molecules 23:1462. https://doi.org/10.3390/molecules23061462

Patel MA, Bhanvase BA, Sonawane SH (2013) Production of cerium zinc molybdate nano pigment by innovative ultrasound-assisted approach. Ultrason Sonochem 20(3):906–913. https://doi.org/10.1016/j.ultsonch.2012.11.008

Raj AES, Mallika C, Swaminathan K, Sreedharan OM, Nagaraja KS (2002) Zinc(II) oxide-zinc(II) molybdate composite humidity sensor. Sens Actuators B Chem 81:229–236. https://doi.org/10.1016/S0925-4005(01)00957-1

Sachuk O, Kopachevska N, Kuznetsova L, Zazhigalov V, Starchevskyy V (2017) Influence of ultrasonic treatmenton the properties of ZnO-MoO_3 oxide system. Chem Chem Technol 11:152–157. https://doi.org/10.23939/chcht11.02.152

Shahri Z, Bazarganipour M, Salavati-Niasari M (2013) Controllable synthesis of novel zinc molybdate rod-like nanostructures via simple surfactant-free precipitation route. Superlattices Microstruct 63:258–266. https://doi.org/10.1016/j.spmi.2013.08.020

Sheng XX, Zhou LZ, Guo XJ, Bai X, Liu XR, Liu JK, Luo CX (2021) Composition design and anticorrosion performance optimization of zinc molybdate pigments. Mater Today Commun 28:102477. https://doi.org/10.1016/j.mtcomm.2021.102477

Tiwari SK, Singh A, Yadav P, Bibek KS, Rolly V, Rout SK, Ela S (2021) Structural and dielectric properties of Cu-doped α-$ZnMoO_4$ ceramic system for enhanced green light emission and potential microwave applications. J Mater Sci: Mater Electron 32:12881–12889. https://doi.org/10.1007/s10854-020-04225-6

Wang D, Huang M, Zhuang Y, Jia H, Sun J, Guan M (2017) Phase- and morphology-controlled synthesis of zinc molybdate for excellent photocatalytic property. Eur J Inorg Chem 42:4939–4946. https://doi.org/10.1002/ejic.201701066

Wang L, Liang W, He S, Liu M, Zhao Y, Zhang W, Chen Y, Lai X, Bi J, Gao D (2020) Realization of superior electrochemical performances for $ZnMoO_4$ anode material through the construction

strategy of 3D flower-like single crystalline. J Alloys Compd 816:152673. https://doi.org/10.1016/j.jallcom.2019.152673

Xue R, Hong W, Pan Z, Jin W, Zhao H, Song Y, Zhou J, Liu Y (2016) Enhanced electrochemical performance of $ZnMoO_4$/reduced grapheme oxide composites as anode materials for lithium-ion batteries. Electrochim Acta 222:838–844. https://doi.org/10.1016/j.electacta.2016.11.045

Yadav P, Sinha E (2019) Structural, photophysical and microwave dielectric properties of a-$ZnMoO_4$ phosphor. J Alloys Compd 795:446–452. https://doi.org/10.1016/j.jallcom.2019.05.019

Zazhigalov VA, Diyuk EA, Sidorchuk VV (2014) Development of VPO catalysts supported on mesoporous modified material based on an aerosol gel. Kinet Catal 55:399–408. https://doi.org/10.1134/S0023158414030148

Zazhigalov VA, Sachuk EV, Kopachevskaya NS, Bacherikova IV, Wieczorek-Ciurowa K, Shcherbakov SN (2016) Mechanochemical synthesis of nanodispersed compounds in the Zno-MoO_3 system. Theor Exp Chem 52:97–103. https://doi.org/10.1007/s11237-016-9456-8

Zazhigalov VA, Sachuk OV, Kopachevska NS, Starchevskyy VL, Sawlowicz Z (2017) Effect of ultrasonic treatment on formation of nanodimensional structures in ZnO–MoO_3 system. Theor Exp Chem 53:53–59. https://doi.org/10.1007/s11237-017-9501-2

Zazhigalov VO, Sachuk OV, Diyuk OA, Kopachevska NS, Starchevskyy VL, Kurmach MM (2019) The effect of ultrasonic treatment on the physical-chemical properties of the ZnO/MoO_3 System. Nanocomposit Nanostruct Appl 221:153–166. https://doi.org/10.1007/978-3-030-17759-1_11

Zhai BG, Mab QL, Yang L, Huang YM (2017a) Growth of $ZnMoO_4$ nanowires via vapor deposition in air. Mater Lett 188:119–1224. https://doi.org/10.1016/j.matlet.2016.11.049

Zhai BG, Ma QL, Yang L, Huang YM (2017b) Synthesis and optical properties of Tb-doped pentazinc dimolybdate pentahydrate. Res Phys 7:3991–4000. https://doi.org/10.1016/j.rinp.2017.10.026

Zhang G, Yu S, Yang Y, Jiang W, Zhang S, Huang B (2010) Synthesis, morphology and phase transition of the zinc molybdates $ZnMoO_4{\cdot}0.8H_2O$/a-$ZnMoO_4$/$ZnMoO_4$ by hydrothermal method. J Cryst Growth 312:1866–1874. https://doi.org/10.1016/j.jcrysgro.2010.02.022

Zhang X, Zhang W, Zeng G, Du J, Zhang W, Yang R (2019) The effect of different smoke suppressants with APP for Enhancing the Flame Retardancy and Smoke Suppression on Vinyl Ester Resin. Polym Eng Sci 60:314–322. https://doi.org/10.1002/pen.25286